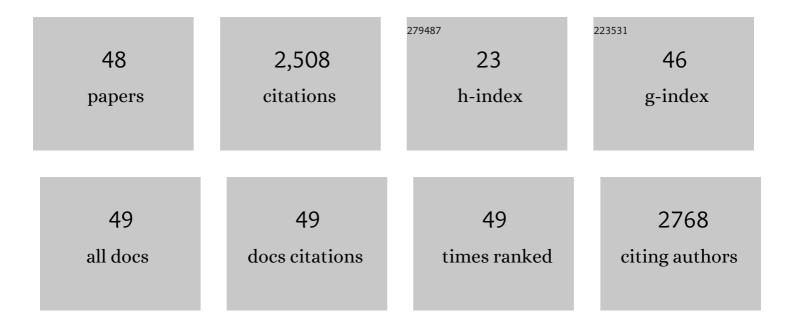
## Chihâ<sup>^</sup>Long Tsai

List of Publications by Year in descending order

Source: https://exaly.com/author-pdf/1486859/publications.pdf Version: 2024-02-01



| #  | Article  | IF  | CITATIONS |
|----|--|-----|-----------|
| 1  | Li <sub>7</sub> La <sub>3</sub> Zr <sub>2</sub> O <sub>12</sub> Interface Modification for Li Dendrite<br>Prevention. ACS Applied Materials & Interfaces, 2016, 8, 10617-10626.  | 4.0 | 632       |
| 2  | Scandium-Substituted<br>Na <sub>3</sub> Zr <sub>2</sub> (SiO <sub>4</sub> ) <sub>2</sub> (PO <sub>4</sub> ) Prepared by a<br>Solution-Assisted Solid-State Reaction Method as Sodium-Ion Conductors. Chemistry of Materials,<br>2016, 28, 4821-4828.                 | 3.2 | 229       |
| 3  | About the Compatibility between High Voltage Spinel Cathode Materials and Solid Oxide Electrolytes<br>as a Function of Temperature. ACS Applied Materials & Interfaces, 2016, 8, 26842-26850.  | 4.0 | 193       |
| 4  | A garnet structure-based all-solid-state Li battery without interface modification: resolving incompatibility issues on positive electrodes. Sustainable Energy and Fuels, 2019, 3, 280-291.   | 2.5 | 133       |
| 5  | Room temperature demonstration of a sodium superionic conductor with grain conductivity in excess of 0.01 S cm <sup>â^'1</sup> and its primary applications in symmetric battery cells. Journal of Materials Chemistry A, 2019, 7, 7766-7776.                        | 5.2 | 129       |
| 6  | High Capacity Garnet-Based All-Solid-State Lithium Batteries: Fabrication and 3D-Microstructure<br>Resolved Modeling. ACS Applied Materials & Interfaces, 2018, 10, 22329-22339.   | 4.0 | 91        |
| 7  | A Novel Sol–Gel Method for Largeâ€Scale Production of Nanopowders: Preparation of<br>Li <sub>1.5</sub> Al <sub>0.5</sub> Ti <sub>1.5</sub> ( <scp>PO</scp> <sub>4</sub> ) <sub>3</sub> as an<br>Example. Journal of the American Ceramic Society, 2016, 99, 410-414. | 1.9 | 79        |
| 8  | Cathode-electrolyte material interactions during manufacturing of inorganic solid-state lithium batteries. Journal of Electroceramics, 2017, 38, 197-206.  | 0.8 | 63        |
| 9  | Thermal stability of Ba(Zr0.8â^'xCexY0.2)O2.9 ceramics in carbon dioxide. Journal of Applied Physics, 2009, 105, 103504.   | 1.1 | 60        |
| 10 | High conductivity of mixed phase Al-substituted Li7La3Zr2O12. Journal of Electroceramics, 2015, 35, 25-32.   | 0.8 | 60        |
| 11 | Electrochemical Performance of All-Solid-State Li-Ion Batteries Based on Garnet Electrolyte Using<br>Silicon as a Model Electrode. ACS Energy Letters, 2018, 3, 1006-1012.   | 8.8 | 58        |
| 12 | Low temperature sintering of fully inorganic all-solid-state batteries – Impact of interfaces on full cell performance. Journal of Power Sources, 2021, 482, 228905.   | 4.0 | 58        |
| 13 | Room-temperature all-solid-state sodium batteries with robust ceramic interface between rigid electrolyte and electrode materials. Nano Energy, 2019, 65, 104040.  | 8.2 | 52        |
| 14 | Orientation dependence and electric-field effect in the relaxor-based ferroelectric crystal(PbMg1/3Nb2/3O3)0.68(PbTiO3)0.32. Physical Review B, 2002, 65, .  | 1.1 | 50        |
| 15 | Dielectric, hypersonic, and domain anomalies of (PbMg1/3Nb2/3O3)1â^'x(PbTiO3)x single crystals. Journal of Applied Physics, 2001, 89, 7908-7916.   | 1.1 | 45        |
| 16 | The influence of water on the electrical conductivity of aluminum-substituted lithium titanium phosphates. Solid State Ionics, 2018, 321, 83-90.   | 1.3 | 44        |
| 17 | Low temperature sintering of Ba(Zr0.8â^'xCexY0.2)O3â^'δ using lithium fluoride additive. Solid State<br>Ionics, 2010, 181, 1083-1090.  | 1.3 | 41        |
| 18 | Insights into the reactive sintering and separated specific grain/grain boundary conductivities of Li1.3Al0.3Ti1.7(PO4)3. Journal of Power Sources, 2021, 492, 229631.   | 4.0 | 40        |

Chihâ<sup>^</sup>'Long Tsai

| #  | Article   | IF  | CITATIONS |
|----|---|-----|-----------|
| 19 | Tortuosity in anode-supported proton conductive solid oxide fuel cell found from current flow rates and dusty-gas model. Journal of Power Sources, 2011, 196, 692-699.          | 4.0 | 36        |
| 20 | On the interfacial charge transfer between solid and liquid Li <sup>+</sup> electrolytes. Physical Chemistry Chemical Physics, 2017, 19, 26596-26605.                           | 1.3 | 33        |
| 21 | Anode-pore tortuosity in solid oxide fuel cells found from gas and current flow rates. Journal of<br>Power Sources, 2008, 180, 253-264.   | 4.0 | 30        |
| 22 | Dendrite-tolerant all-solid-state sodium batteries and an important mechanism of metal self-diffusion.<br>Journal of Power Sources, 2020, 476, 228666.                          | 4.0 | 26        |
| 23 | Reactions of garnet-based solid-state lithium electrolytes with water — A depth-resolved study. Solid State Ionics, 2018, 320, 259-265.   | 1.3 | 24        |
| 24 | Chemical Environment-Induced Mixed Conductivity of Titanate as a Highly Stable Oxygen Transport<br>Membrane. IScience, 2019, 19, 955-964.                                       | 1.9 | 23        |
| 25 | Water-based fabrication of garnet-based solid electrolyte separators for solid-state lithium batteries.<br>Green Chemistry, 2020, 22, 4952-4961.                                | 4.6 | 23        |
| 26 | All-ceramic Li batteries based on garnet structured<br>Li <sub>7</sub> La <sub>3</sub> Zr <sub>2</sub> O <sub>12</sub> . Materials Technology, 2020, 35, 656-674.               | 1.5 | 22        |
| 27 | Phases and Domain Structures in Relaxor-Based Ferroelectric (PbMg1/3Nb2/3O3)0.69(PbTiO3)0.31Single<br>Crystal. Japanese Journal of Applied Physics, 2001, 40, 4118-4125.        | 0.8 | 20        |
| 28 | Enhancing the performance of high-voltage LiCoMnO4 spinel electrodes by fluorination. Journal of Power Sources, 2017, 341, 122-129.   | 4.0 | 20        |
| 29 | Compatibility study towards monolithic self-charging power unit based on all-solid thin-film solar module and battery. Journal of Power Sources, 2017, 365, 303-307.            | 4.0 | 17        |
| 30 | Challenges regarding thin film deposition of garnet electrolytes for all-solid-state lithium batteries with high energy density. Ionics, 2018, 24, 2199-2208.                   | 1.2 | 15        |
| 31 | Fabrication, Performance, and Model for Proton Conductive Solid Oxide Fuel Cell. Journal of the<br>Electrochemical Society, 2011, 158, B885.                                    | 1.3 | 14        |
| 32 | Flexible All-Solid-State Li-Ion Battery Manufacturable in Ambient Atmosphere. ACS Applied Materials<br>& Interfaces, 2020, 12, 37067-37078.                                     | 4.0 | 14        |
| 33 | Single-Ion-Conducting "Polymer-in-Ceramic―Hybrid Electrolyte with an Intertwined NASICON-Type<br>Nanofiber Skeleton. ACS Applied Materials & Interfaces, 2021, 13, 61067-61077. | 4.0 | 14        |
| 34 | Instability of Ga-substituted Li <sub>7</sub> La <sub>3</sub> Zr <sub>2</sub> O <sub>12</sub> toward metallic Li. Journal of Materials Chemistry A, 2022, 10, 10998-11009.      | 5.2 | 14        |
| 35 | Hypersonic and dielectric properties of (PbZn1/3Nb2/3O3)0.915–(PbTiO3)0.085 single crystal. Journal of<br>Applied Physics, 2000, 87, 2327-2330.                                 | 1.1 | 13        |
| 36 | Performance and stability of a liquid anode high-temperature metal–air battery. Journal of Power<br>Sources, 2014, 247, 749-755.  | 4.0 | 13        |

Chihâ<sup>^</sup>'Long Tsai

| #  | Article  | IF  | CITATIONS |
|----|--|-----|-----------|
| 37 | Atomic-scale investigation of Na3V2(PO4)3 formation process in chemical infiltration via in situ transmission electron microscope for solid-state sodium batteries. Nano Energy, 2021, 87, 106144.                     | 8.2 | 12        |
| 38 | Influence of titanium nitride interlayer on the morphology, structure and electrochemical performance of magnetron-sputtered lithium iron phosphate thin films. Journal of Power Sources, 2015, 281, 326-333.          | 4.0 | 11        |
| 39 | Impact of Fluorination on Phase Stability, Crystal Chemistry, and Capacity of LiCoMnO <sub>4</sub><br>High Voltage Spinels. ACS Applied Energy Materials, 2018, 1, 715-724.  | 2.5 | 10        |
| 40 | Engineering of Sn and Preâ€Lithiated Sn as Negative Electrode Materials Coupled to Garnet Taâ€LLZO Solid<br>Electrolyte for Allâ€Solidâ€State Li Batteries. Batteries and Supercaps, 2020, 3, 557-565.                 | 2.4 | 10        |
| 41 | Ionic Conductivity of Na <sub>3</sub> V <sub>2</sub> P <sub>3</sub> O <sub>12</sub> as a Function of<br>Electrochemical Potential and its Impact on Battery Performance. Batteries and Supercaps, 2021, 4,<br>479-484. | 2.4 | 10        |
| 42 | Thermal stability of 5†V LiCoMnO4 spinels with LiF additive. Solid State Ionics, 2018, 320, 378-386.   | 1.3 | 8         |
| 43 | Active Interphase Enables Stable Performance for an Allâ€Phosphateâ€Based Composite Cathode in an<br>Allâ€Solidâ€State Battery. Small, 2022, 18, e2200266.   | 5.2 | 7         |
| 44 | Effect of lithium fluoride on thermal stability of proton-conducting Ba(Zr0.8â^`xCexY0.2)O2.9 ceramics. Solid State Ionics, 2010, 181, 1654-1658.  | 1.3 | 6         |
| 45 | Field-cooled-zero-field-heated and zero-field-heated dielectric behaviors of<br>(Pbmg1/3Nb2/3O3)0.67(PbTiO3)0.33single crystal. Ferroelectrics, Letters Section, 2000, 27, 125-135.                                    | 0.4 | 4         |
| 46 | Protonic and Electronic Conduction in Proton Conductive Solid Oxide Fuel Cells. Materials Research<br>Society Symposia Proceedings, 2011, 1330, 40501.   | 0.1 | 1         |
| 47 | Feasibility and Limitations of High-Voltage Lithium-Iron-Manganese Spinels. Journal of the Electrochemical Society, 2022, 169, 070518.   | 1.3 | 1         |
|    |  |     |           |

48 Determination of Anode-Pore Tortuosity from Gas and Current Flow Rates in SOFCs. , 0, , 127-140.

0